sciendo

Research Article

Mokhtar Messaad, Messoud Bourezane, Mohamed Latrache, Amina Tahar Berrabah, and Djamel Ouzendja*

Three-dimensional seismic analysis of concrete gravity dams considering foundation flexibility

https://doi.org/10.2478/mme-2021-0012
Received May 19, 2021; accepted Aug 02, 2021

Abstract: Concrete dams are considered as complex construction systems that play a major role in the context of both economic and strategic utilities. Taking into account reservoir and foundation presence in modeling the dam-reservoir-foundation interaction phenomenon leads to a more realistic evaluation of the total system behavior. The article discusses the dynamic behavior of dam-reservoir-foundation system under seismic loading using Ansys finite element code. Oued Fodda concrete dam, situated at Chlef, in North-West of Algeria, was chosen as a case study. Parametric study was also performed for different ratios between foundation Young's modulus and dam Young's modulus E_f/E_d (which varies from 0.5 to 4). Added mass approach was used to model the fluid reservoir. The obtained results indicate that when dam Young's modulus and foundation Young's modulus are equal, the foundation soil leads to less displacements in the dam body and decreases the principal stresses as well as shear stresses.

Keywords: Concrete gravity dam, dynamic soil-structure interaction, finite element method, flexible foundation, stiffness similarity, young's modulus

1 Introduction

Over the years, the seismic behavior of concrete gravity dams has been a topic of interest for many dam engineers. Several researches have been conducted to determine the behavior of the dams against the seismic loads. Generally, the seismic analysis of structures often relies on the hypotheses that the foundation, which is subjected to horizontal acceleration, is rigid. The response of the soil to the motion of the structure and the response of the structure to the motion of the soil is known as Soil–Structure Interaction (SSI), presented by Wolf [1]. The simplified response spectrum method is proposed by Fenves and Chopra [2] to perform preliminary design and evaluation of concrete gravity sections. In this method, a standard fundamental mode of vibration that is representative of typical sections is used. This mode shape does not take into account the foundation flexibility since it is representative of a standard concrete gravity section on rigid foundation.

Several factors can affect the dynamic behavior of concrete dams to seismic loads, including the dam-foundation and dam-reservoir interaction. In numerous studies, a reasonable assumption based on massless foundation was used to evade the aforementioned considerations for structures built on rock, such as concrete dams [3–18].

To reduce the damage of dams during an earthquake, many researchers have been trying to determine the effects of the soil–structure interaction. An indirect boundary element method, which uses Green's function for nonlinear soil–structure interaction analysis for a surface foundation in time domain, was formulated by Wolf and Obernhuber [19]. Based on a study that considers contact elements at dam-foundation interaction surface, Ouzandja *et al.* have obtained the nonlinear three dimensional seismic response of concrete gravity dam in relation to Oued Fodda [20]. Based on the substructure method, a procedure of a linear dynamic analysis was developed in order to determine the seismic response of arch dams and simulated using EACD-3D-96 program. The procedure allows both (1) three-dimensional analysis of a concrete arch dam-water–foundation system and (2) hydrodynamic pressure waves' partial absorption by sediments in the reservoir boundary-bottom and sides. Considering the flexibility, inertia, and the damping of the foundation in concrete dams' dynamic response, Tan and Chopra implemented substruc-

***Corresponding Author: Djamel Ouzendja:** Laboratory of Materials and Mechanics of Structures (lmms), University of Msila, Algeria; Email: dj_ouzandja@yahoo.com
Mokhtar Messaad: Laboratory of Hydraulic Developments and Environment LAHE, University of Biskra, Biskra, Algeria
Messoud Bourezane: Department of Civil Engineering and Hydraulics, University of Biskra, Biskra, Algeria
Mohamed Latrache: Faculty of Technology Mohamed Khieder, Universty of Biskra, BP 145 RP, 07000 Biskra, Algeria
Amina Tahar Berrabah: Department of Civil Engineering, Smart Structures Laboratory, University of Ain Temouchent, Algeria

ture method and they came to the conclusion that inertia and damping affect responses when compared with the massless foundation [21–23]. Hokmabadi et al. evaluated the seismic response of mid-rise buildings affected by SPSI. Both analytical and shaking table studies were carried out on FB structures, shallow foundation structures, and floating pile foundation structures [24, 25]. By investigating the effects of varied input mechanisms of earthquake on dams' seismic response, Leger and Boughoufalah came to the conclusion that there are advantages and disadvantages of using four earthquake input mechanisms [26]. In a frequency domain linear analysis, Fenves and Chopra [27] investigated the dam-reservoir-foundation interaction system while Gaun [28] has described an affective numerical procedure in order to investigate the dynamic response of a reservoir-dam-foundation system directly in the time domain. Ghaemian *et al.* stated that the shape and mass of the foundation effects on arch dams' linear response are significant [29]. A "standard" massless foundation model presents the dam-foundation interaction effects [30]. In the study by the USACE, it is hypothesized that the displacement at the base of the foundation disappears and roller supports are vertically put on the foundation's sides. Considering the hydrodynamic reservoir pressure, Ghaedi *et al.* studied the effect of shapes and sizes of openings in the Kinta RCC dam. The results indicated that around openings, there are considerable stresses and cracks under hydrodynamic pressure [31]. By implementing the coupled FE-BE method, Khalili and Valliappan formulated a computational method for the transient soil-structure interaction analysis, in which the structure was simulated using FEM and the half space was modeled by the BEM [32]. In a single step, soil and structure are included and analyzed in a single model within the direct approach. Concerning the substructure approach, the Soil–Structure Interaction system is divided into three varied parts. Also, the response of one substructure is utilized as an input in the analysis of the following substructure. In order to determine the linear response of the dam-reservoir system, Westergaard presented an approach based on a number of masses added to the dam body. In this approach, he assumes that there is equivalence between the hydrodynamic effect on the dam and the inertial force caused by the sum of the added masses [33].

This study aims at enriching the studies related to the seismic response of concrete gravity dams. A three-dimensional finite element model is used to investigate the effects of foundation flexibility and dam-reservoir-foundation interaction on the seismic response of concrete gravity dam. For this purpose, the Oued Fodda concrete gravity dam in Chlef, North-west Algeria, is selected as a case study. The hydrodynamic pressure of the water reservoir is modeled as an added mass using the Westergaard approach. The effect of foundation flexibility has been obtained by taking into account various dam-foundation rock interaction ratios. One of these ratios is expressed as: modulus of elasticity of foundation (EF)/modulus of elasticity of dam concrete (ED). The varied numerical analyses are modeled by using the ANSYS program [34].

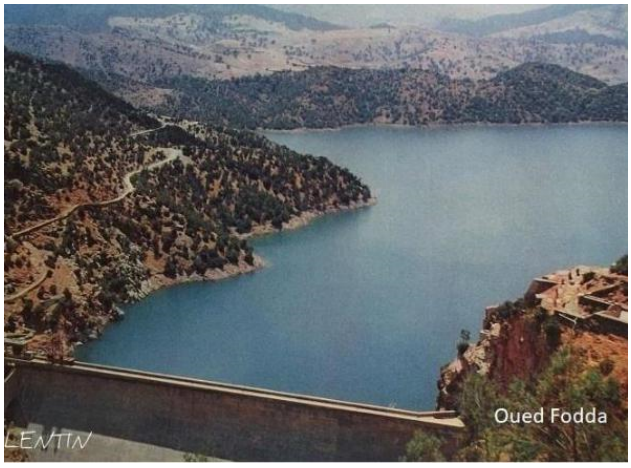

Figure 1: View of Oued Fodda concrete gravity dam.

2 Mathematical model of the soil-structure system

For the purpose of developing the basic dynamic equilibrium equations of the soil-structure interaction, we consider the soil-structure system shown in Figure 2.

$$U = v + u$$

U: Absolute displacement
v: Added displacements
u: Free field displacements

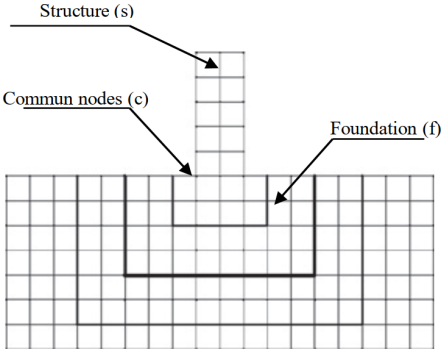

Figure 2: Soil-structure interaction model.

We consider that the SSI model is divided into three sets of nodes. The common nodes of structure interface and the base are identified with (c); the nodes in the structure are the nodes (s); and the other nodes in the foundation are the (f) nodes. The equilibrium of the system's dynamic force is given in terms of absolute displacements (U) in the following equation:

$$\begin{bmatrix} M_{ss} & 0 & 00 & M_{cc} & 0 \\ 0 & 0 & M_{ff} & & \end{bmatrix} \begin{bmatrix} \ddot{U}_s \\ \ddot{U}_c \\ \ddot{U}_f \end{bmatrix} + \begin{bmatrix} K_{ss} & K_{sc} & 0 \\ K_{cs} & K_{cc} & K_{cf} \\ 0 & K_{fc} & K_{ff} \end{bmatrix} \begin{bmatrix} U_s \\ U_c \\ U_f \end{bmatrix} = \begin{bmatrix} 0 \\ 0 \\ 0 \end{bmatrix} \tag{1}$$

in which the mass and the stiffness at the common nodes are the sum of the contribution of the structure (s) and the foundation (f), and it is presented by:

$$M_{cc} = M_{cc}^{(s)} + M_{cc}^{(f)} \quad K_{cc} = K_{cc}^{(s)} + K_{cc}^{(f)} \tag{2}$$

In terms of absolute motion, there are no external forces affecting the system. However, the displacements at the foundation borders must be known. To avoid solving this SSI problem directly, the dynamic response of the unstructured foundation is calculated. In many cases, the solution in free-field can be obtained from a simple one-dimensional site model.

The three-dimensional solution in free-field is denoted by the absolute displacements (V) and the absolute accelerations ($\ddot{u}$). By a simple change in variables, it is now possible to express the absolute displacements (U) and the accelerations ($\ddot{U}$) in terms of displacements u relatively with displacements in free-field v, in which:

$$\begin{bmatrix} U_s \\ U_c \\ U_f \end{bmatrix} = \begin{bmatrix} u_s \\ u_c \\ u_f \end{bmatrix} + \begin{bmatrix} v_s \\ v_c \\ v_f \end{bmatrix} \qquad \begin{bmatrix} \ddot{U}_s \\ \ddot{U}_c \\ \ddot{U}_f \end{bmatrix} = \begin{bmatrix} \ddot{u}_s \\ \ddot{u}_c \\ \ddot{u}_f \end{bmatrix} + \begin{bmatrix} \ddot{v}_s \\ \ddot{v}_c \\ \ddot{v}_f \end{bmatrix} \tag{3}$$

Eq. (1) can be now written as the following equation:

$$\begin{bmatrix} M_{ss} & 0 & 0 \\ 0 & M_{cc} & 0 \\ 0 & 0 & M_{ff} \end{bmatrix} \begin{bmatrix} \ddot{u}_s \\ \ddot{u}_c \\ \ddot{u}_f \end{bmatrix} + \begin{bmatrix} K_{ss} & K_{sc} & 0 \\ K_{cs} & K_{cc} & K_{cf} \\ 0 & K_{fc} & K_{ff} \end{bmatrix} \begin{bmatrix} u_s \\ u_c \\ u_f \end{bmatrix} = - \begin{bmatrix} M_{ss} & 0 & 0 \\ 0 & M_{cc} & 0 \\ 0 & 0 & M_{ff} \end{bmatrix} \begin{bmatrix} \ddot{v}_s \\ \ddot{v}_c \\ \ddot{v}_f \end{bmatrix} - \begin{bmatrix} K_{ss} & K_{sc} & 0 \\ K_{cs} & K_{cc} & K_{cf} \\ 0 & K_{fc} & K_{ff} \end{bmatrix} \begin{bmatrix} v_s \\ v_c \\ v_f \end{bmatrix} = R \tag{4}$$

If the displacement v_c in free-field is constant on the structure base, the term v_s represents the rigid body motion of the structure. Therefore, Eq. (4) can be also simplified by the fact that the rigid body's static motion of the structure is:

$$\begin{bmatrix} K_{ss} & K_{sc} \\ K_{cs} & K_{cc}^{(s)} \end{bmatrix} \begin{bmatrix} v_s \\ v_c \end{bmatrix} = \begin{bmatrix} 0 \\ 0 \end{bmatrix} \tag{5}$$

In addition, the dynamic motion of free-field of the foundation requires that:

$$\begin{bmatrix} M_{cc}^{(f)} & 0 \\ 0 & M_{ff} \end{bmatrix} \begin{bmatrix} \ddot{v}_c \\ \ddot{v}_f \end{bmatrix} + \begin{bmatrix} K_{cc}^{(f)} & K_{cf} \\ K_{cf} & K_{ff} \end{bmatrix} \begin{bmatrix} v_c \\ v_f \end{bmatrix} = \begin{bmatrix} 0 \\ 0 \end{bmatrix} \tag{6}$$

Therefore, the right side of Eq. (4) can be written as:

$$R = \begin{bmatrix} M_{ss} & 0 & 0 \\ 0 & M_{cc}^{(f)} & 0 \\ 0 & 0 & 0 \end{bmatrix} \begin{bmatrix} \ddot{v}_s \\ \ddot{v}_c \\ 0 \end{bmatrix} \tag{7}$$

Hence, the right side of Eq. (4) does not contain the mass of the foundation. Therefore, the three-dimensional dynamic equilibrium equation for the soil-structure system with added damping will be in the following form:

$$[M]\{\ddot{u}\} + [C]\{\dot{u}\} + [K]\{u\} = -[m_x]\,\ddot{v}_x(t) - [m_y]\,\ddot{v}_y(t) - [m_z]\,\ddot{v}_z(t) \tag{8}$$

in which $[M]$, $[C]$, and $[K]$ are the mass, damping, and stiffness matrices of the model, respectively. The added relative displacements $\{u\}$ exist for the soil-structure system and must be zeroed on the foundation's sides and bottom. The terms $\ddot{v}_x(t)$, $\ddot{v}_y(t)$, and $\ddot{v}_z(t)$ are the acceleration components in free-field if the structure is not present. The columns matrices $[m_i]$ are the direction masses for the added structure only.

3 Hydrodynamic pressure effect

The hydrodynamic pressure effect is considered according to the added mass technique which was initially proposed by Westergaard [33]. Assuming that the water reservoir is nonviscous, incompressible, and its motion is of small amplitude, the equation which expresses the hydrodynamic pressure can be stated as follows:

$$\nabla^2 P = 0 \tag{9}$$

The solution of this equation is proposed by Westergaard and is used in the current work to calculate the hydrodynamic pressure imposed on the upstream face of the dam body during an earthquake.

4 Finite elements dam-foundation system modeling

The dimensions of the dam-reservoir-foundation system are instantiated in Figures 3 and 4:

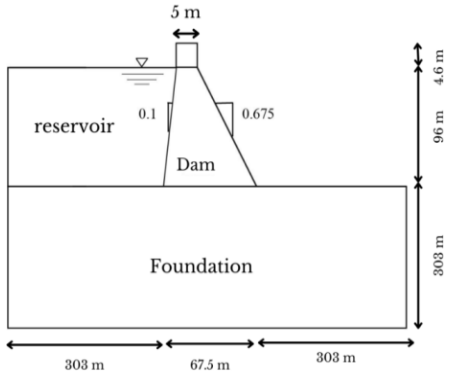

Figure 3: Transverse section and dimensions.

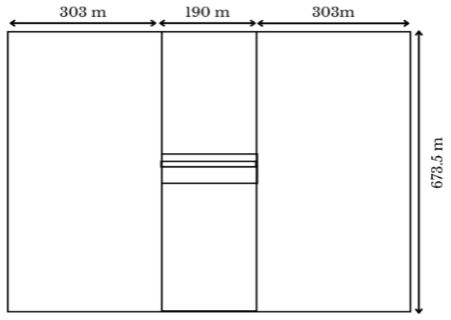

Figure 4: Top view and dimensions.

Oued Fodda dam was selected in the current article as a case study. The height of the dam is 101 m, its width at the top of the crest is 5 m, and at the base it is 67.5 m. The dam is assumed to be homogeneous and elastic linear with the following properties: modulus of elasticity E_d = 24.6 × 109 N/m^2, Poisson's ratio ν = 0.2, and density ρ_d = 2640 kg/m^3. However, the material properties of the foundation are as follows: modulus of elasticity E_f = 20 × 109 N/m^2, Poisson's ratio ν = 0.33, and density ρ_f = 2000 kg/m^3. The foundation's modulus of elasticity varies from 0.5 to 4.0 times of the dam's modulus of elasticity as considered in the literature [35, 36]. In addition, because of space and in order to better illustrate the possible differences in behavior, only the results for different ratios (E_f/E_d = 0.5, 1, 1.5, 3, 4) are considered for assessment of performance.

A three-dimensional (3D) discretization by finite elements (Figure 5) is used for modeling the dam-foundation system. This finite element model is simulated using Ansys software [34]. Ansys is considered as one of the leading commercial finite element programs in the world.

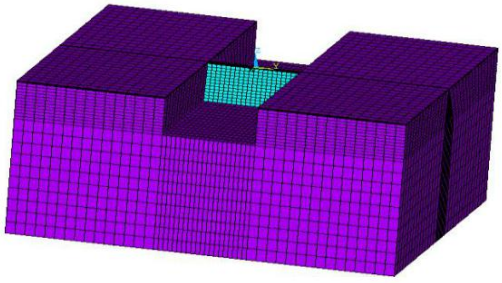

Figure 5: Finite element discretization of the dam-foundation system.

The solid finite elements (Solid185) used in the analysis to model dam body and the foundation has four nodes and 2 × 2 × 2 integration points. A three-dimensional (3D) finite element model with 39,750 solid finite elements (Solid185) is used to model Oued Fodda dam and the foundation soil, while 900 finite element model (SURF154) is used to model the reservoir water. Generally, concrete dams having viscous damping ratios of 2–5% are accepted [37]. The damping for the entire structural system is modeled by Rayleigh damping. In this current work, a Rayleigh damping of 5% is imposed to both the dam and the foundation.

5 Dynamic analysis

5.1 Modal analysis

The lowest five natural frequencies of the dam-foundation system along with mode shapes of the dam's fundamental mode for the different ratios (E_f/E_d) are presented in Tables 1–5 and Figures 6–10, respectively:

Table 1: First five natural frequencies of the dam-foundation with E_f/E_d = 0.5.

Mode	Frequency (Hz)	Period (s)
1	2.19	0.456
2	2.24	0.446
3	2.27	0.440
4	2.45	0.408
5	2.52	0.396

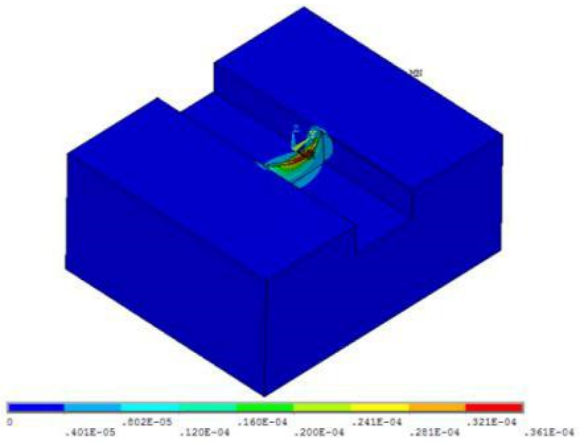

Figure 6: Mode shape of the dam's fundamental mode with E_f/E_d = 0.5.

Table 2: First five natural frequencies of the dam-foundation with E_f/E_d = 1.

Mode	Frequency (Hz)	Period (s)
1	2.72	0.36
2	3.11	0.321
3	3.16	0.316
4	3.4	0.294
5	3.45	0.289

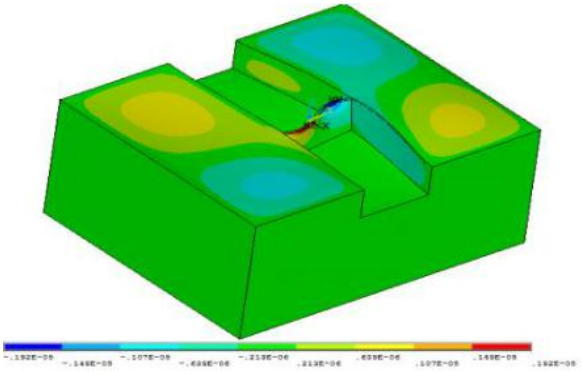

Figure 7: Mode shape of the dam's fundamental mode with E_f/E_d = 1.

Table 3: First five natural frequencies of the dam-foundation with E_f/E_d = 1.5.

Mode	Frequency (Hz)	Period (s)
1	2.87	0.348
2	3.79	0.263
3	3.87	0.258
4	4.13	0.242
5	4.17	0.239

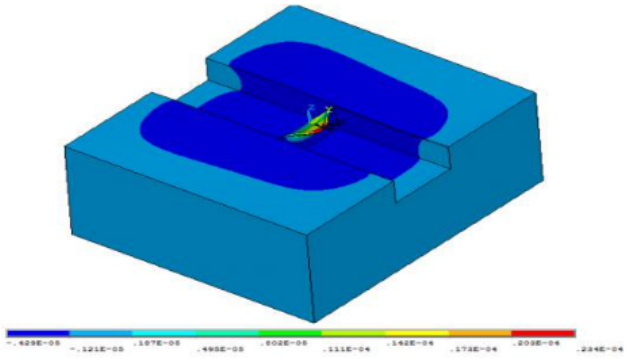

Figure 8: Mode shape of the dam's fundamental mode with E_f/E_d = 1.5.

Table 4: First five natural frequencies of the dam-foundation with E_f/E_d = 3.

Mode	Frequency (Hz)	Period (s)
1	3.02	0.331
2	4.35	0.229
3	5.32	0.187
4	5.44	0.183
5	5.74	0.174

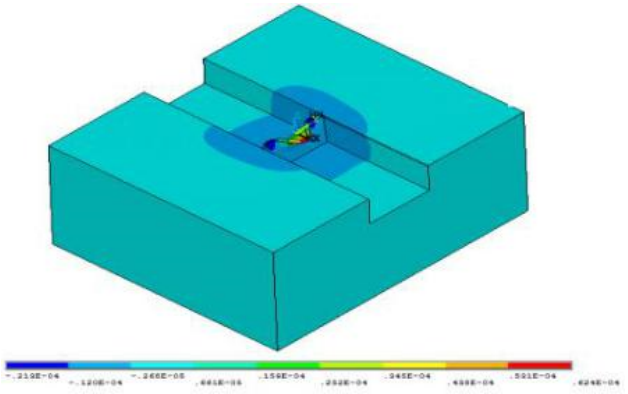

Figure 9: Mode shape of the dam's fundamental mode with E_f/E_d = 3.

Table 5: First five natural frequencies of the dam-foundation with E_f/E_d = 4.

Mode	Frequency (Hz)	Period (s)
1	3.06	0.326
2	4.38	0.228
3	6.03	0.165
4	6.13	0.163
5	6.23	0.160

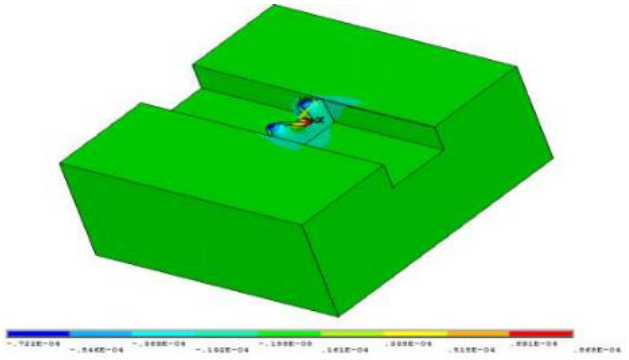

Figure 10: Mode shape of the dam's fundamental mode with E_f/E_d = 4.

According to the results shown in Tables 1–5, it is clear that the frequencies vary from one ratio to another. The higher the ratio is, the bigger the frequencies are. For the case of the dam with the lowest foundation rigidity, the frequencies are lower than those for the dam with higher foundation rigidity. This is due to the fact that the stiffness matrix is located at the numerator of the frequency formula. This means that stiffness increasing leads to frequency increasing and vice versa.

5.2 Transient analysis

The horizontal component of the 1980 El Asnam earthquake acceleration scaled by factor of 2.5 is used in the analyses (Figure 11). In 1980, El Asnam province was subjected to a strong earthquake (M7). We only have a record of a replica of this earthquake with peak ground acceleration (PGA) 0.132 g. Therefore, we selected the record of replica earthquake with a scaling factor of 2.5 to get an earthquake acceleration record with PGA 0.33 g almost equal to PGA of record of the strong earthquake (M7).

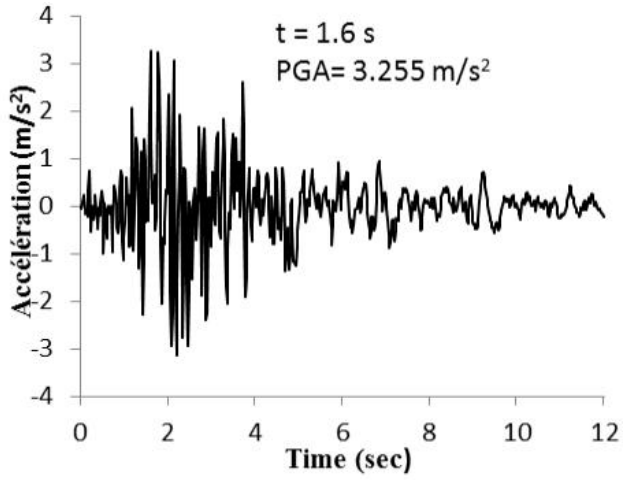

Figure 11: Time history of horizontal acceleration for 1980 El Asnam earthquake record scaled by factor of 2.5.

5.2.1 Horizontal displacements

Figure 12 demonstrates the time history of horizontal displacement at the dam crest in upstream face for dam with different ratio E_f/E_d cases:

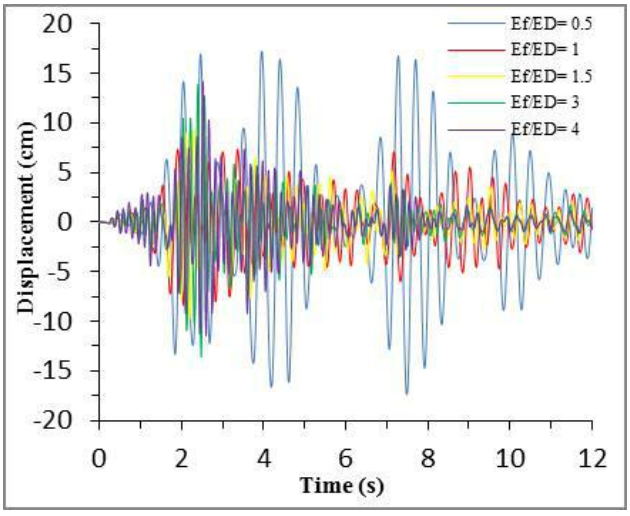

Figure 12: Variation of horizontal displacement at dam crest.

From Figure 12, it is obvious that the displacement values differ from one ratio to another. The maximum horizontal displacements at the crest point are higher, reaching 17.2 cm and 14.1 cm with E_f/E_d ratios 0.5 and 4, respectively. The displacements decrease at ratios 1.5 and 3, in which they reach 9.22 cm and 13.8 cm, respectively. However, the displacements are lower and reach 7.3 cm in the case of ratio E_f/E_d = 1. We can conclude that the displacements are greater when the dam Young's modulus and the foundation Young's modulus are different. The results of modal analysis can be also used to interpret this observation. The mode shapes of fundamental modes support the obtained results. It is noticeable that the displacements are lower when dam Young's modulus and foundation Young's modulus are equal.

Figure 13 shows a comparison of displacements according to the height of the dam for the different cases studied.

Figure 13 displays that in the cases of the dam with foundation ratios 0.5 and 4, the values for maximum horizontal displacement at the crest are 17.2 cm and 14.1 cm, respectively, while in the case of the dam with the foundation

ratio 1, it is 7.3 cm. This indicates that there is approximately 57% and 48% decrease in the amplitude of displacement at the peak. It should be recognized that the foundation ratio ($E_f/E_d = 1$) has a significant impact on dam displacements.

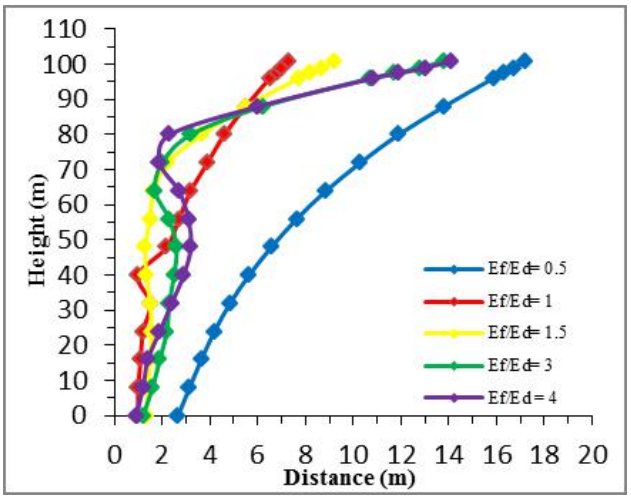

Figure 13: Horizontal displacement of the dam for the different studied cases.

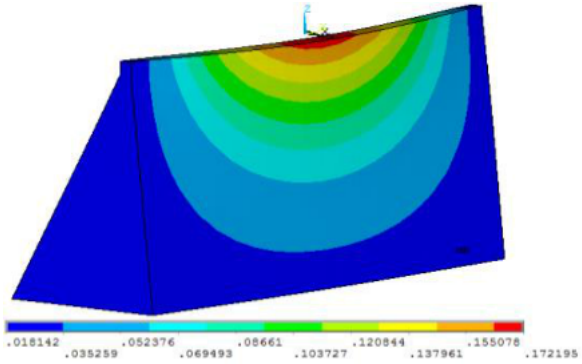

Figure 14: Maximum horizontal displacement contours of the dam with $E_f/E_d = 0.5$.

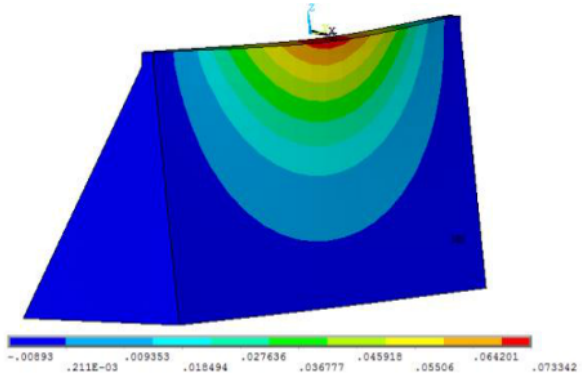

Figure 15: Maximum horizontal displacement contours of the dam with $E_f/E_d = 1$.

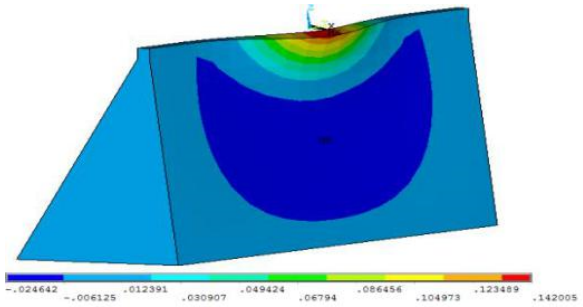

Figure 16: Maximum horizontal displacement contours of the dam with $E_f/E_d = 1$.

Figures 14, 15, and 16 represent the maximum horizontal displacement contours of the dam for the ratio values 0.5, 1, and 4, respectively.

According to Figures 14–16, it is clear that the maximum displacements occur at the middle region of the dam crest.

5.2.2 Variation of stresses

Figures 17 and 18 show stresses along the height due to the variation in the upstream maximum principal tensile and compressive face of the dam.

Numerical analyses illustrate that the maximum principal stresses become greater at the height of 70 m of the dam. The maximum principal tensile stresses reach 16,703.8 kN/m^2, 32,932 kN/m^2, and 33,160 kN/m^2 with the ratios 1.5, 3, and 4, respectively; while the compressive stresses are −15632.4 kN/m^2, −32112 kN/m^2, and −35703 kN/m^2. In addition, the maximum principal ten-

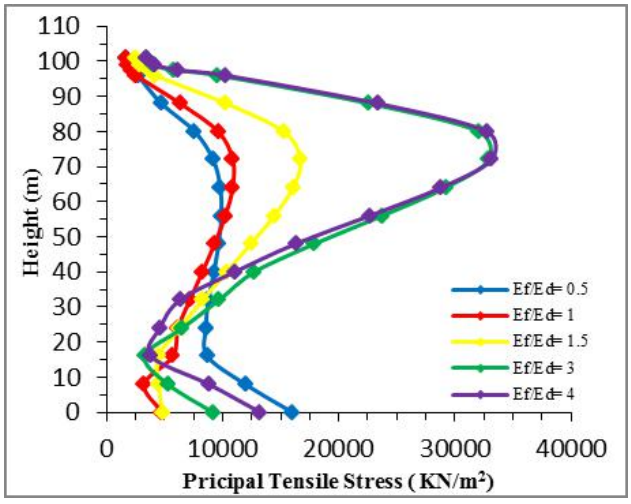

Figure 17: Maximum principal tensile stresses along the dam height.

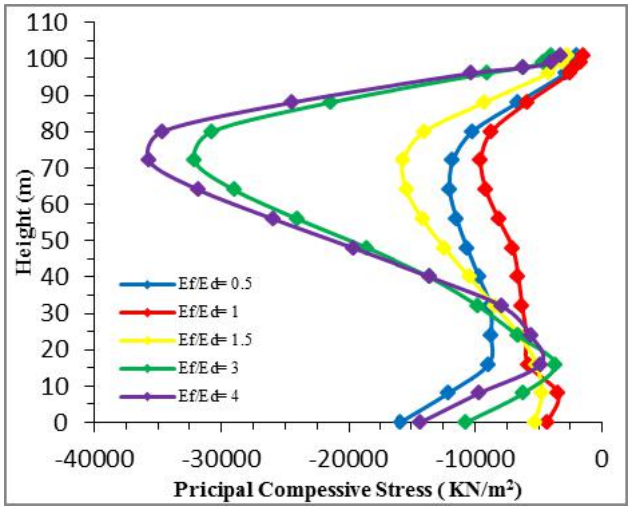

Figure 18: Maximum principal compressive stresses along the dam height.

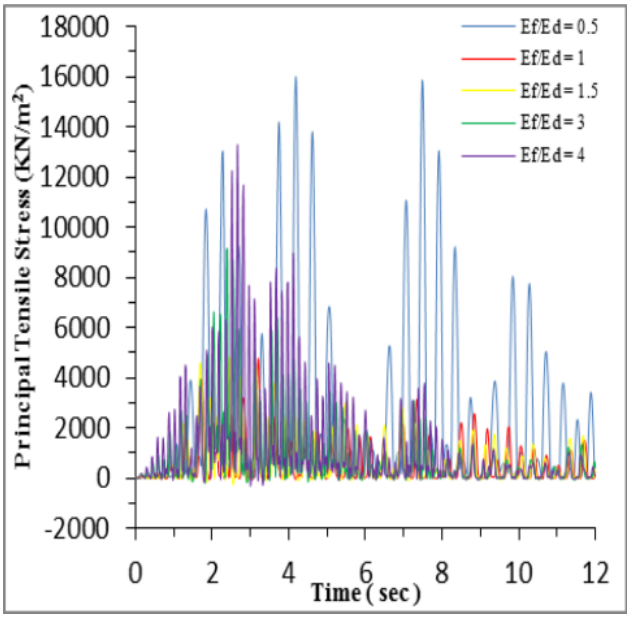

Figure 19: Time history for principal tensile stress at dam heel.

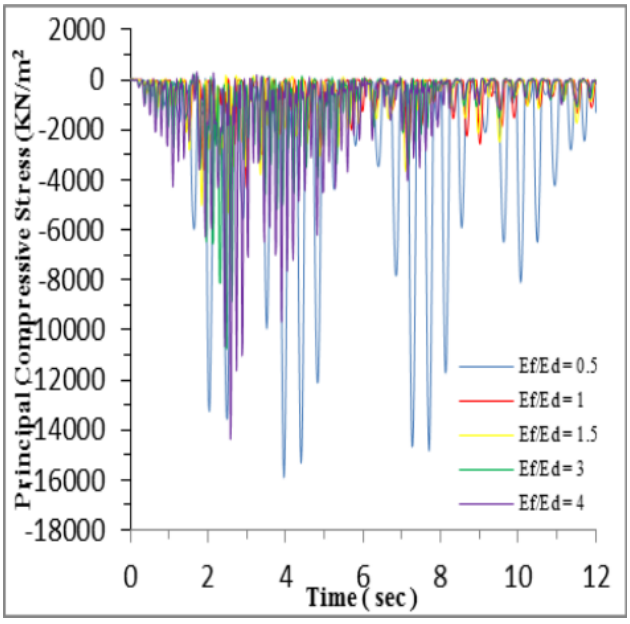

Figure 20: Time history for principal compressive stress at dam toe.

sile and compressive stresses decrease to 10,870 kN/m^2 and –9521 kN/m^2, respectively, with ratio of 1.

On the other hand, at the dam's base, the maximum principal tensile and compressive stresses are higher at the ratio of 0.5 than the other ratios, reaching 16,406.1 kN/m^2 and –15,899 kN/m^2, respectively. However, maximum principal stresses are lower at the ratio of 1, at which they reach 4767.7 kN/m^2 and –4303.4 kN/m^2. It is obvious that the principal tensile and compressive stresses are lower at the ratio of 1. This is due to the stiffness similarity of both the dam and the foundation.

Figures 19 and 20 show time history for principal tensile stresses at dam heel and principal compressive stresses at dam toe.

Figures 19 and 20 show the time history for both principal tensile stresses at dam heel and the principal compressive stresses at dam toe for different ratios. For the principal tensile stresses, it is noticeable that they decrease from 16,406.1 KN/m^2 and 13,253.8 KN/m^2 for the ratios 0.5 and 4, respectively, to 4767.7 KN/m^2 for ratio 1. This signifies that there is an approximate decrease of 71% and 64% in the magnitude of the principal tensile stresses at dam heel. For the principal compressive stresses, on the other hand, they are –15,899.3 KN/m^2 and –14,296.1 KN/m^2 for the ratios 0.5 and 4, while they decrease to –4303.4 KN/m^2 for the ratio 1. It means that there is a decrease of 72% and 69% in the magnitude of principal compressive stresses. It is observed that the principal tensile and compressive stresses decrease when the ratio 1 is taken into account. This refers to the fact that the dam and foundation have similar stiffness.

Figures 21–23 represent the maximum principal tensile stress contours of the dam for the three ratios 0.5, 1, and 4.

From Figures 21–23, it is obvious that the maximum principal tensile stresses occur at the dam's base for the ratio 0.5, while they occur at the dam body's chest for the two rest ratios.

Figure 24 shows the time history of shear stress at heel in different ratios.

Figure 24 shows the time history for principal shear stress at dam heel for different ratios. The shear stresses are 437.2 KN/m^2 and 412.8 KN/m^2 for the ratios 3 and 4, respectively. However, the shear stresses increase to 707.8 KN/m^2

and 679.6 KN/m^2, respectively, for the ratios 0.5 and 1.5 while it is 540.2 KN/m^2 for the ratio 1. For the structure on foundation with ratios 3 and 4, the seismic acceleration gives rise to a moment of overturning and transverse shear. As the rock is very stiff, these two stress resultants will not lead to any additional deformation or rocking motion at the base. For the structure founded on soil with ratio 0.5, the motion of the base of the structure will be different from the free-field motion because of the coupling of the structure-soil system.

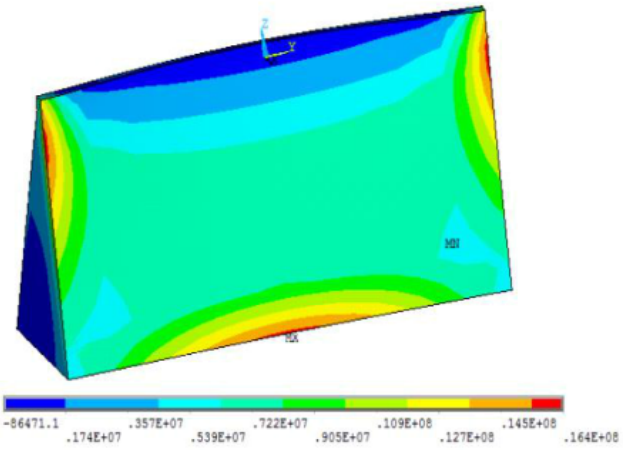

Figure 21: Maximum principal tensile stress contours of the dam with $E_f/E_d = 0.5$.

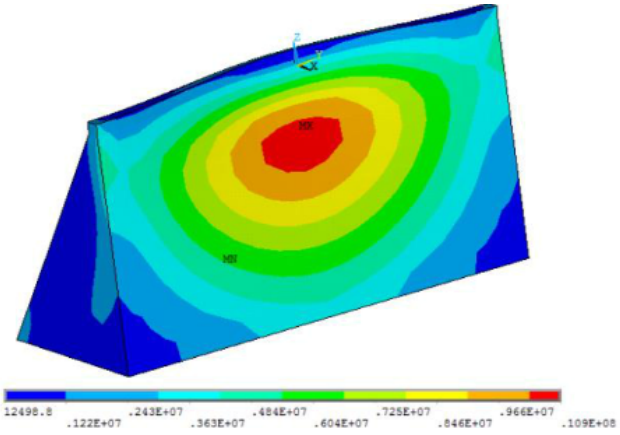

Figure 22: Maximum principal tensile stress contours of the dam with $E_f/E_d = 1$.

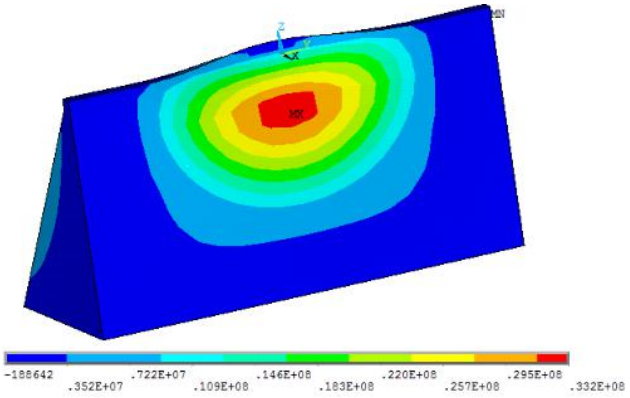

Figure 23: Maximum principal tensile stress contours of the dam with $E_f/E_d = 1$.

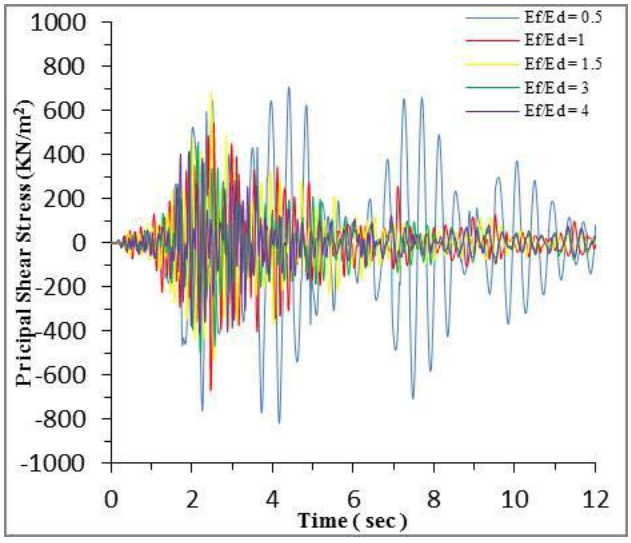

Figure 24: Time history for principal shear stress at dam heel.

6 Conclusions

The current study attempts to identify the effects of the foundation's flexibility on the seismic response of a concrete gravity dams. On the basis of the obtained results, the following conclusions can be drawn:

- For the case of the dam with the lowest foundation rigidity, the frequencies are usually lower than those for the case of the dam with higher foundation rigidity.
- The displacements are lower when dam Young's modulus and foundation Young's modulus are equal compared to the case when they are different.
- The foundation ratio ($E_f/E_d = 1$) has a significant impact on dam displacements, in which the displacements decrease.
- The maximum horizontal displacements at the crest reach its highest magnitude for the ratio 0.5 and 4.
- The stiffness similarity of both the dam and the foundation decreases the principal tensile and compressive stresses.

- The principal tensile and compressive stresses are greater at the ratios 3 and 4, at the height of 70 m of the dam.
- The principal tensile and compressive stresses are higher at the ratio 0.5 at the dam's base.
- The maximum principal stresses are lower at the ratio of 1 at both the dam's base and at the height of 70 m.
- For the structure on rigid foundation where the rock is very stiff, the resultant shear stresses will not lead to any additional deformation or rocking motion at the base.
- The stiffness similarity of the foundation should be considered in the numerical analyses to evaluate the critical response of the dam-foundation system.
- The case of the stiffness similarity of both the dam and the foundation is more conservative than the case when the stiffness differs.

The stiffness similarity of the dam and the foundation is more excited than the case when the stiffness differs, which is justified by the difference in stresses and displacements for the different cases under study. Therefore, the stiffness similarity of the dam and the foundation should be taken into account in the modeling of the dam-foundation interaction phenomenon to achieve more reliable results.

Acknowledgement: The authors wish to thank the doctor in the Department of Civil Engineering at University of Ain Temouchent (Algeria), Dr. AMINA ATTIA, for his profound support.

References

[1] **Wolf J. P.:** Dynamic Soil-Structure Interaction, Prentice Hall: Englewood Cliffs, NJ, **1985.**

[2] **Fenves, G., & Chopra, A. K.:** Earthquake analysis of concrete gravity dams including reser-voir bottom absorption and dam-water-foundation rock interaction. Earthquake engineering & structural dynamics, 12(5), 663-680, **1984**. https://doi.org/10.1002/eqe.4290120507

[3] **Leger, P., & Boughoufalah, M.:** Earthquake input mechanisms for time-domain analysis of dam—foundation systems. Engineering Structures, 11(1), 37-46, **1989.** https://doi.org/10.1016/0141-0296(89)90031-X

[4] **Bayraktar, A., Hancer, E., & Akköse, M.**: Influence of base-rock characteristics on the stochastic dynamic response of dam–reservoir–foundation systems. Engineering Structures, 27(10), 1498-1508, **2005.** https://doi.org/10.1016/j.engstruct.2005.05.004

[5] **Long, Y., Zhang, C., & Xu, Y.:** Nonlinear seismic analyses of a high gravity dam with and without the presence of reinforcement. Engineering Structures, 31(10), 2486-2494, **2009.** https://doi.org/10.1016/j.engstruct.2009.06.004

[6] **Bayraktar, A., Altunişik, A. C., Sevim, B., Kartal, M. E., Türker, T., & Bilici, Y.:** Comparison of near-and far-fault ground motion effect on the nonlinear response of dam–reservoir–foundation systems. Nonlinear Dynamics, 58(4), 655-673, **2009.** https://doi.org/10.1007/s11071-009-9508-x

[7] **Akköse, M., & Şimşek, E.:** Non-linear seismic response of concrete gravity dams to near-fault ground motions including dam-water-sediment-foundation interaction. Applied Mathe-matical Modelling, 34(11), 3685-3700, **2010.** https://doi.org/10.1016/j.apm.2010.03.019

[8] **Bayraktar, A., Türker, T., Akköse, M., & Ateş, Ş.:** The effect of reservoir length on seismic performance of gravity dams to near- and far-fault ground motions. Natural Hazards, 52(2), 257-275, 2010. https://doi.org/10.1007/s11069-009-9368-1

[9] **Sevim, B., Altunşik, A. C., Bayraktar, A., Akköse, M., & Calayir, Y.:** Water length and height effects on the earthquake behavior of arch dam-reservoir-foundation systems. KSCE Journal of Civil Engineering, 15(2), 295-303, **2011**. https://doi.org/10.1007/s12205-011-0815-7

[10] **Wang, H., Feng, M., & Yang, H.:** Seismic nonlinear analyses of a concrete gravity dam with 3D full dam model. Bulletin of Earthquake Engineering, 10(6), 1959-1977, **2012.** https://doi.org/10.1007/s10518-012-9377-4

[11] **Seyedpoor, S. M., Salajegheh, J., & Salajegheh, E.:** Shape optimal design of materially nonlinear arch dams including dam-water-foundation rock interaction using an improved PSO algorithm. Optimization and engineering, 13(1), 79-100, **2012.** https://doi.org/10.1007/s11081-011-9156-0

[12] **Ardebili, M. H., & Mirzabozorg, H.:** Effects of near-fault ground motions in seismic per-formance evaluation of a symmetric arch dam. soil mechanics and foundation engineering, 49(5), 192-199, **2012**. https://doi.org/10.28991/cej-2019-03091289

[13] **Zhang, S., & Wang, G.:** Effects of near-fault and far-fault ground motions on nonlinear dynamic response and seismic damage of concrete gravity dams. Soil Dynamics and Earthquake Engineering, 53, 217-229, **2013**. https://doi.org/10.1016/j.soildyn.2013.07.014

[14] **Pan, J., Xu, Y., Jin, F., & Zhang, C.:** A unified approach for long-term behavior and seismic response of AAR-affected concrete dams. Soil Dynamics and Earthquake Engineering, 63, 193-202, **2014.** https://doi.org/10.1016/j.soildyn.2014.03.018

[15] **Wang, G., Wang, Y., Lu, W., Zhou, C., Chen, M., & Yan, P.**: XFEM based seismic poten-tial failure mode analysis of concrete gravity dam–water–foundation systems through incre-mental dynamic analysis. Engineering Structures, 98, 81-94, **2015.** https://doi.org/10.1016/j.engstruct.2015.04.023

[16] **Amina, T. B., Mohamed, B., André, L., & Abdelmalek, B.:** Fluid–structure interaction of Brezina arch dam: 3D modal analysis. Engineering Structures,84, 19-28, **2015.** https://doi.org/10.1016/j.engstruct.2014.11.011

[17] **Hariri-Ardebili, M. A., Seyed-Kolbadi, S. M., & Kianoush, M. R.**: FEM-based parametric analysis of a typical gravity dam considering input excitation mechanism. Soil Dynamics and EarthquakeEngineering,84, 22-43, **2016**. https://doi.org/10.1016/j.soildyn.2016.01.013

[18] **Hariri-Ardebili, M. A., Seyed-Kolbadi, S. M., Saouma, V. E., Salamon, J., & Rajagopalan, B.:** Random finite element method for the seismic analysis of gravity dams. Engineering Structures,171, 405-420, **2018.** https://doi.org/10.1016/j.engstruct.2018.05.096

[19] **Wolf, J. P., & Obernhuber, P.**: Non-linear soil-structure-interaction analysis using dynamic stiffness or flexibility of soil in the time domain. Earthquake Engineering & Structural Dynam-ics, 13(2), 195–212, **1985**. https://doi.org/10.1002/eqe.4290130205

[20] **Ouzandja, D., Tiliouine, B., & Ouzandja, T.:** Nonlinear Seismic Response of Concrete Gravity Dams. Sustainable Civil Infrastructures, 13–21, **2017.** https://doi.org/10.1007/978-3-319-61905-7_2

[21] **Tan, H., & Chopra, A. K.:** Earthquake analysis of arch dams including dam-water-foundation rock interaction. Earthquake engineering & structural dynamics, 24(11), 1453-1474, **1995.** https://doi.org/10.1002/eqe.4290241104

[22] **Tan, H., & Chopra, A. K.:** Dam-foundation rock interaction effects in earthquake response of arch dams. Journal of Structural Engineering, 122(5), 528-538, **1996.** https://doi.org/10.1061/(ASCE)07339445(1996)122:5(528)

[23] **Chopra, A. K.:** Earthquake analysis of arch dams: factors to be considered. Journal of Structural Engineering, 138(2), 205-214, **2012.** https://doi.org/10.1061/(ASCE)ST.1943-541X.0000431

[24] **Hokmabadi, A. S., Fatahi, B., & Samali, B.**: Assessment of soil–pile–structure interaction influencing seismic response of mid-rise buildings sitting on floating pile foundations. Com-puters and Geotechnics,55, 172-186, **2014.** https://doi.org/10.1016/j.compgeo.2013.08.011

[25] **Hokmabadi, A. S., Fatahi, B., & Samali, B.:** Physical modeling of seismic soil-pile-structure interaction for buildings on soft soils. International Journal o f Geomechanics, 15(2), 04014046, **2015.** https://doi.org/10.1061/(ASCE)GM.19435622.0000396

[26] **Leger, P., & Boughoufalah, M.:** Earthquake input mechanisms for time-domain analysis of dam—foundation systems. Engineering Structures, 11(1), 37-46, **1989**. https://doi.org/10.1016/0141-0296(89)90031-X

[27] **Fenves, G., & Chopra, A. K.:** Effects of reservoir bottom absorption and dam-water-foundation rock interaction on frequency response functions for concrete gravity dams. Earthquake Engineering & Structural Dynamics, 13(1),13-31, **1985**. https://doi.org/10.1002/eqe.4290130104

[28] **Guan, F., Moore, I. D., & Lin, G.:** Transient response of reservoir–dam–soil systems to earthquakes. International journal for numerical and analytical methods in geomechanics, 18(12), 863-880, **1994.** https://doi.org/10.1002/nag.1610181204

[29] **Ghaemian, M., Noorzad, A., & Moghaddam, M. M.:** Foundation effect on seismic response of concrete arch dams including dam-reservoir interaction. EUROPEAN EARTHQUAKE ENGINEERING, 19(3), 49, **2005.**

[30] **US. Army Corps of Engineers (USACE).:** "Time-History Dynamic Analysis of Concrete Hydraulic Structures;" Chapter 2- Analytical Modeling of Concrete Hydraulic Structures, Chapter 3-Time-History Numerical Solution Techniques", EM 1110-2-6051, **2003.**

[31] **Ghaedi, K., Jameel, M., Ibrahim, Z., and Khanzaei, P.:** Seismic analysis of Roller Com-pacted Concrete (RCC) dams considering effect of sizes and shapes of galleries. KSCE Journal of Civil Engineering, 20 (1), 261-272, **2016.** https://doi.org/10.1007/s12205-015-0538-2

[32] **Yazdchi, M., Khalili, N., & Valliappan, S.:** Dynamic soil–structure interaction analysis via coupled finite-element–boundary-element method. Soil Dynamics and Earthquake Engineer-ing, 18(7), 499-517, **1999.** https://doi.org/10.1016/S0267-7261(99)00019-6

[33] **Westergaard, H. M.:** Water pressures on dams during earthquakes. Transactions of the American society of Civil Engineers, 98(2), 418-433, **1933.** https://doi.org/10.1061/taceat.0004496

[34] **ANSYS.** Theory user's manual, Swanson Analysis Systems Inc, Houston, PA, USA, **2012.**

[35] **Moussaoui, S. E., and Tiliouine, B.:** Etude de l'effet de l'interaction dynamique sur le com-portement sismique du barrage de l'Oued Fodda. In Colloque International sur la vulnérabilité, 11 –12 Octobre 2003, Alger, Algérie, **2003.**

[36] **Yazdchi M., Khalili N., and Valliappan S.:** (1999). "Dynamic soil–structure interaction analysis via coupled finite element–boundary-element method", Soil Dynamics and Earthquake Engineering, 18, 499–517.2888, **1999.** https://doi.org/10.1016/S0267-7261(99)00019-6

[37] **Dreher, K. J.:** Seismic analysis and design considerations for concrete dams, Proceedings of a Conference Held at the Institution of Civil Engineering, London, on 1-2 October 1980, Thomas TelfordLimited, **1981**. https://doi.org/10.1680/dae.01237.0022

[38] **Swaddiwudhipong, S., Lu, H. R., & Wee, T. H.:** Direct tension test and tensile strain ca-pacity of concrete at early age. Cement and concrete research,33(12),2077-2084, **2003.** https://doi.org/10.1016/S0008-8846(03)00231-X

[39] **Sutherland B.:** Experimental and analytical analysis of the stress-strain diagram of frp-confined concrete with different loading rates, M.S. Thesis, Department of Civil Engineering, Kansas State University, USA, **2006.**